water

MDPI

Article

Modelling Trace Metals in River and Sediment Compartments to Assess Water Quality

Aline Grard * and Jean-François Deliège *

FOCUS Research Unit—Freshwater and OCeanic Sciences Unit of Research, PeGIRE Laboratory, Aquapôle Research Center, Faculty of Sciences, Department of Biology, Ecology and Evolution, University of Liège, Allée de la Découverte 11, Building B53, Quartier Polytech 1, 4000 Liège, Belgium

* Correspondence: a.grard@uliege.be (A.G.); jfdeliege@uliege.be (J.-F.D.); Tel.: +32-4-366-23-53 (A.G. & J.-F.D.)

Abstract

The present study focuses on the dynamics of trace metals (TM) in two European rivers, the Mosel and the Meuse. A deterministic description of hydro-sedimentary processes has been performed. The model used to describe pollutant transport and dilution at the watershed scale has been enhanced with the implementation of the MicMod sub-model. The objective of this study is to characterise the dynamics of TM in the water column and bed sediment. A multi-class grain size representation has been developed in MicMod. The dissolved and particulate TM phases have been calculated with specific partitioning coefficients associated with each suspended sediment (SS) class. The processes involved in TM fate have been calibrated in MicMod, including settling velocity, TM releases from the watershed (point and diffuse loads), etc. Following the calibration of the parameters involved in TM transport within the river ecosystem, the main goal is to describe TM dynamics using a pressure–impact relationship model. It was demonstrated that the description of at least one class of fine particles is necessary to obtain an adequate representation of TM concentrations. The focus of this study is low flow periods, which are characterised by the presence of fine particles. The objective is to gain a deeper understanding of the processes that control the transport of TM. This paper establishes consistent pressure–impact relationships between TM loads (urban, industrial, soils) from watersheds and concentrations in rivers.

Keywords: water quality modelling; trace metal; grain size; suspended sediment; partitioning coefficient; hydro-sedimentary processes

Academic Editor: Bommanna Krishnappan

Received: 23 May 2025
Revised: 20 June 2025
Accepted: 21 June 2025
Published: 24 June 2025

Citation: Grard, A.; Deliège, J.-F. Modelling Trace Metals in River and Sediment Compartments to Assess Water Quality. *Water* **2025**, *17*, 1876. https://doi.org/10.3390/w17131876

1. Introduction

Trace metals are naturally present in the aquatic environment through bedrock erosion and weathering processes [1–3]. In the last decade, studies have been dedicated to understanding water chemistry [4,5] associated with anthropogenic loads and natural contributions from different lithologies in watersheds. The budgets of trace metal sources are described in [6], including river particulate metal fluxes from natural soil erosion.

Fluxes of anthropogenic and natural pollutants connect the watershed and the associated watercourses [7–9]. Among these pollutants, trace metals, in contrast to many other types of pollutants, are highly persistent in sediments, since they cannot be degraded and provide a delayed source of contamination to the river through leaching and erosion [3,10]. The potential ecological risk of each TM in sediments is determined by its total content and speciation. The partitioning of TM in water is difficult to predict because it depends on a

variety of additional factors associated with anthropogenic metal inputs, such as (i) pollution origin; (ii) concentration and characteristics of suspended, colloidal, and dissolved ligands; and (iii) changes in the physico-chemical parameters of water [11]. TM bound to SS are transported with the flow but may also be deposited on the riverbed. Deposited material may itself be subsequently eroded and resuspended. The association of TM and SS varies according to several factors, including the chemical composition of the water and the SS.

We propose to analyse the spatio-temporal dynamics of metal contamination along two major rivers in Western Europe (the French part of the Mosel River watershed and the Belgian Meuse River), using a modelling tool. Validation was carried out by comparing calculated concentrations (and resulting fluxes) with observations.

The improvement of sediment quality in the most recent years in Europe and the decrease in metal concentrations since the 1970s [12] reflect the decisive role of environmental policies, such as more efficient wastewater treatments and local applications of the Water Framework Directive, WFD 2000/60/EC [13].

To assess metal pollution in river sediments, monitoring programs have been implemented in watercourses, with variable measurement frequencies. The monitoring of sediment quality and metal concentrations under the supervision of Water Basin Agencies in several countries of Western Europe has produced a large amount of data on the liquid and solid phases in the rivers, from local to international scales, under the supervision of international commissions for the Rhine, Meuse, and Scheldt rivers [12,14,15].

The advantages and benefits of modelling are (i) its capacity to provide continuous values (concentrations and fluxes) in space and time, (ii) its forecasting capacity at small and large scales (once validated), (iii) its lower cost than monitoring programs, and (iv) its predictive ability to simulate scenarios (i.e., management plans).

In this paper, we investigate TM modelling (dissolved and particulate phases) in the water column of the river ecosystem. We aim to calibrate not only partitioning coefficients of trace metals [16] but also settling velocities of different particle size classes, estimation of trace metal releases from the watershed, etc. The goals of this paper were to (1) calibrate parameters involved in equations describing trace metals transport and behaviour in the river ecosystem, (2) describe trace metals dynamics with a pressure–impact relationship model, and (3) strengthen the accuracy by validation on other datasets. This modelling supplements the monitoring network with (i) calculated values for non-monitored rivers and (ii) continuous spatio-temporal maps of concentrations and fluxes, in order to provide useful support for water quality management [17], i.e., the European Water Framework Directive 2000/60/EC [13].

2. Material and Methods

2.1. Study Sites Description and Dataset

Two continental rivers of Western Europe were selected based on the availability of monitoring data and required data for the modelling (urban data, wastewater treatment plants information, industrial releases, discharges, etc.). They are transboundary rivers flowing from France to the North: the Meuse River flows from France to Belgium and the Netherlands [18]; the Mosel River flows from France to Germany.

The Meuse River (950 km) was studied and modelled in its Belgian part (middle part of the watershed). Its entire catchment (Figure 1) has a surface area of 34,564 km^2 [19]. There are 624 rivers, 5561 km of simulated linear rivers, and 24,779 calculation nodes. The study site was the Eijsden monitoring station, located at the Belgo–Dutch border at the 617 km point. At this point, the modelled Meuse and its tributaries have a catchment area of 20,554 km^2.

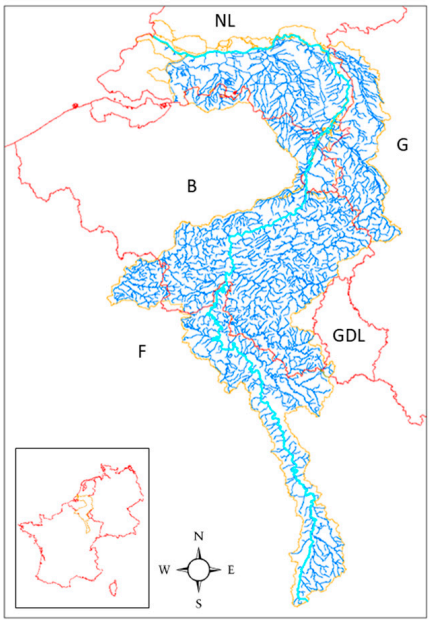

Figure 1. Map of the International River Basin District of the Meuse (France (F), Belgium (B), GD Luxembourg (GDL), Germany (G), the Netherlands (NL)). The Meuse River is marked by a light blue line; deep blue lines represent tributaries; red lines are the borders; and yellow line is the International River Basin District boundary. The projection system is Belgian Lambert 72 (LB72).

The Mosel River (544 km) was studied and modelled in its French part (upstream part of the watershed). Its entire catchment (the Mosel River and its tributaries, Figure 2) has a surface area of 28,286 km^2 [20]. There are 331 rivers, 4380 km of simulated linear rivers, and 20,238 calculation nodes. At the French outlet, the Mosel has a catchment area of 11,280 km^2. The study site was the monitoring station located at Liverdun (Mosel, 193.5 km).

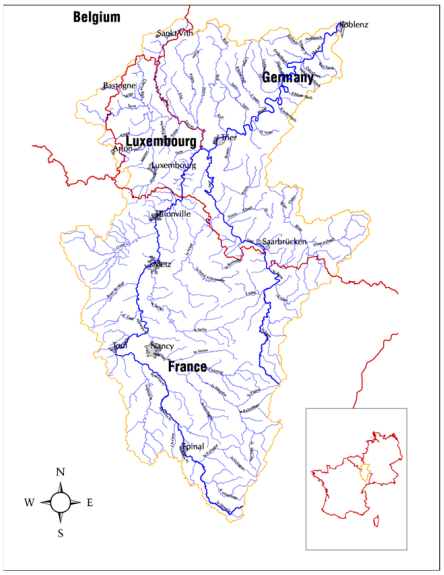

Figure 2. Map of the Mosel–Saar Transnational Basin (France, GD Luxembourg, and Germany). The Mosel (to the West) and Saar (to the East) rivers are marked by dark blue lines; light blue lines represent tributaries; red lines are the borders; and the yellow line is the International Mosel–Saar Basin boundary. The projection system is the European Terrestrial Reference System 1989–Lambert Azimuthal Equal Area (ETRS89-LAEA).

These river systems are mainly influenced by oceanic climate and are characterised by high flows in winter, with occurrences of flash floods, and low flows in late summer [12]. At the Eijsden monitoring station, the Meuse has a characteristic low discharge (i.e., daily discharge not reached more than 10 days per year—2.7th percentile, 10/365), estimated to be 30.9 m^3/s [21]. The average annual discharge was 250.5 m^3/s [21]. The largest recorded daily discharge was 1590.1 m^3/s. The Meuse is a typical lowland river, heavily equipped for navigation and flood protection in the last 390 km (Belgian and Dutch parts). The Mosel is characterised by a low flow (i.e., the monthly minimum flow reached once in five years; statistical flow that gives information on the severity of the low flow) at the French outlet of about 31.6 m^3/s [22]. The average annual discharge was 111.8 m^3/s at Uckange, 282 km away from the source [23]. The largest recorded daily discharge was 1090.0 m^3/s. The 2.7th percentile was estimated to be 11.9 m^3/s. The Mosel is canalised from Nancy (150 km downstream of its source), and its watershed is mainly agricultural and forested. Urban and industrial areas are developed in the downstream part of the basin [20,24]. In this context, the year 2020 was used for the Meuse and the Mosel simulations.

In this work, two metals, copper (Cu) and zinc (Zn), are characterised by contrasting adsorption and desorption behaviours. Copper exhibits a significant dissolved fraction, whereas zinc is mainly transported in particulate form [10,25]. For the Meuse and Mosel basins, copper and zinc are inventoried as pollutant substances with a high toxic risk, and their fluxes are among the ten largest emitted ones in the Rhine–Meuse basin [26]. We decided to focus on copper and zinc for the investigated basins. Trace metals and suspended sediment data are available and used for the Meuse [21] and Mosel [27] for the year 2020. These data were largely described in [16]. The modelling allowed us to calculate anthropogenic fluxes of trace metals at the outlets of the two studied watersheds (Table 1).

Table 1. Simulated fluxes of Cu and Zn (kg/year) at the outlets of the Meuse and Mosel watersheds (TM-d: Dissolved TM; TM-t: Total TM).

	Meuse Fluxes (2020) kg/y	**Mosel Fluxes (2020) kg/y**
Cu-d	576	826
Cu-t	1000	1555
Zn-d	1830	3091
Zn-t	5980	8928

2.2. Methodology

The Pegase model [17,28,29] is a one-dimensional unsteady hydrological model operating at the watershed scale (from a few square kilometres to more than one hundred thousand square kilometres). The characterisation of transport and dilution, by applying the principle of mass–balance relationships, has enabled the establishment of explicit and consistent pressure–impact relationships between the loads discharged from the watersheds and the concentrations of pollutants in the river. The specificity of the model is its ability to work at a high spatial resolution not only for small river basins (water body level) but also for large drainage networks (>100,000 km^2). It is a process-oriented, physically based model. It consists of a set of partial differential equations describing the evolution in space and time of selected state variables: flow rate, temperature, concentrations of pollutants, nutrients, oxygen, and biological populations [29]. The evolution of fluxes from the watershed induced changes in the aquatic ecosystem responses, which are explicitly characterised by the model.

The model presented here is deterministic and physically based and proposes a detailed representation of physicochemical processes controlled by environmental conditions.

It is based on a set of kinetic equations representing the dynamics of the system and the evolution of biological processes. Models of this kind are often opposed to more empirical models based on a much simpler representation of process kinetics (e.g., QUAL2K [30], WASP [31], AQUATOX [32]).

It has been demonstrated that, due to specific processes implied in TM behaviour, namely their interaction with sediments, the riverbed can act as a secondary TM source (or sink) through the process of erosion (or sedimentation) [10,14,33,34]. Modelling allows for the establishment of balances between ecosystem compartments in the water column (water and SS) and bed sediment. Due to their different behaviours, SS characterisation (organic matter, metal oxides, clay, etc.) is essential, and many studies have described SS into different classes [35].

The Cu and Zn loads from the described watersheds [21,27] were integrated into the databases used (and provided) by the administrations (the Walloon Administration, SPW, and the Rhin Meuse Water Agency, AERM): urban, industrial, wastewater treatment plants, etc. These datasets were used to (i) calibrate the newly developed *Mic*ropollutant *Mod*elling (MicMod) sub-model, which describes specific processes involving TM, such as adsorption, desorption, sedimentation, resuspension, etc; and (ii) perform TM simulations. The calibration processes were specific to partitioning coefficients, SS settling velocities, TM urban emission rates, and soil leaching functions (also referred to as diffuse loads) in the investigated watersheds. The values assigned to the calibrated parameters used in the simulations are presented in Table 2.

Table 2. Overview of the calibrated parameters and assigned values in the present modelling.

Input Parameter	Units	Value
Urban emission rates	mg/PE/d	
Cu		8.5
Zn		10.0
Soil loads functions	mg/m^3	
Diss. Cu		1.0
Part. Cu		0.5
Diss. Zn		4.0
Part. Zn		2.5
Settling velocities	m/s	
Clay		9.3×10^{-6}
Fine silt		1.2×10^{-5}
Coarse silt		2.3×10^{-5}

The partitioning coefficients for copper and zinc were calibrated for the Meuse and Mosel basins [16]. Estimation of urban emission rates was approached using methods reported in the literature [6,26,29,36]. Diffuse loads are due to livestock farming activities and diffuse loads from soils. These loads can be estimated using semi-statistical functions that are region-specific. These parameters were found to be both sensitive and critical for the modelling of TM and SS within the river ecosystem. It is important to note that settling velocities are the only relevant parameters for the calibration of SS concentrations. The values for clay, fine silt, and coarse silt were calibrated in the French Mosel watershed. This step is a prerequisite for later simulations, the results of which should demonstrate a significant effect of grain size distribution on the fate of TM in rivers.

2.3. Model Implementation

Modelling suspended sediment concentrations is a critical issue for trace metal characterisation [37,38]. Furthermore, the chemical composition and physical properties of SS during high flow may be very different from those during low flow [10,39]. Consequently, transport by advection and dispersion, as well as erosion and sedimentation, are essential processes driving the fate of SS.

Generally, TM concentrations in sediments (SS and bed sediment [BS]) are mainly influenced by fine particles [12,14,40]. The smaller the particle size, the higher the surface area/volume ratio (and also the surface area/weight ratio); the concentration of trace metals in sediments (expressed in mg/kg) is therefore higher for smaller particles.

Particulate matters in rivers play an important role in controlling trace metal speciation. In MicMod, the particulate phase is represented by a multi-class system. There are N + 1 classes, where N is parameterisable. Organic suspended matter is considered separately from mineral suspended matter due to its possible degradation in the water column [17,29]. This representation is integrated into the operational model by the POMD method [41]. Common models such as WASP and QUAL2K take into account trace metals in river systems, but they do not consider the fractional distribution of suspended sediment. The multi-class system of particulate phase in MicMod constitutes a significant advantage over most traditional approaches.

Four distinct classes of particles were used to simulate the heterogeneity of SS with respect to erosion and sedimentation: from the "very fine" SS fraction, which has a very low settling velocity either because of its size or its density, towards "coarser" classes in which SS are more prone to sedimentation, reaching the river system during higher flow conditions. The four classes of mineral suspended sediment are considered in the MicMod sub-model, according to [16], which compiled data from [42–45]: mean diameters for clay (d_{moy} = 1 µm), fine silt (d_{moy} = 9 µm), coarse silt (d_{moy} = 40 µm), and sand (d_{moy} = 157 µm). This sub-model is implemented in the Pegase model in order to (i) characterise the transport and fate of TM (dissolved and particulate phases) in a river ecosystem and (ii) describe the Cu and Zn pressure–impact relationships. These improvements will strengthen the model as an operational management tool, compliant with the requirements of European Water Framework Directive 2000/60/EC (WFD).

The MicMod sub-model is composed of the main processes involving sediments (suspended sediments expressed in g/m^3 and bed sediments expressed in g/m^2) and micropollutants in a river ecosystem [16]. Two separate compartments are considered: (i) sediment concentration due to deposition and (ii) sediment concentration due to resuspension, for each particle size class. The principle of sediment conservation is respected: the temporal variation in sediment content within a compartment equals the difference between sedimentation and resuspension [46].

The chemical forms (bound complexes, free ions, etc.) of trace metals are controlled by the physicochemical and biological characteristics of the aquatic environment. Their mobility, transportation, and partitioning in natural river systems involve very complex processes that depend on the physicochemical properties of the contaminants, water, and sediments [47].

The solid–solution distribution of trace metals was quantified using the partitioning coefficient, K_d, a general concept described in the literature [10,48], and expressed as

$$K_d = C_{ss}/C_w$$

where C_{ss} is the metal particulate concentration per mass (mg/kg) and C_w is the dissolved metal concentration per volume (mg/m^3). K_d depends on the abundance and speciation of

elements in materials. Elevated K_d values indicate that elements have a high affinity for solid phases, whereas elements with low K_d values are more easily weathered, removed in soil solution and/or groundwater, and transported in dissolved phases in the river [48]. For a given element, the K_d may depend on several environmental factors, including the time required to reach equilibrium, the nature of particles, the concentration of complexing ligands, the particle concentration, and even biological activity [49,50].

The Cu and Zn partitioning coefficients calculated according to grain sizes (clay, fine silt, and coarse silt) at Eijsden [16] have been used in the environmental modelling dedicated to the assessment of water quality.

Adsorption, desorption, sedimentation, resuspension, and discharges from the watershed are described as first-order processes in the deterministic, physically based Pegase model [28,46,51] (Supplementary Materials, Equation (S1)).

3. Results and Discussion

3.1. Calibration of Specific Parameters Involved in Equations Describing TM Behaviour

One of the objectives of this study is to provide an analysis of the calibration process for critical parameters and processes within a deterministic aquatic ecosystem model. The MicMod sub-model requires a large amount of data to calculate TM concentrations in the river ecosystem. The following parameters need to be calibrated: (i) urban emission rates, (ii) soil load functions, and (iii) settling velocity by SS class (in order to describe the TM transport and behaviour in the water column, in interaction with the bed layer). The calibration of metal partitioning coefficients between (i) SS and water column and (ii) BS and water column was realised in [16] and is partly discussed in this paper.

3.1.1. Urban Emission Rates

The study sites are exposed to urban anthropogenic pressures. The rivers are characterised by high levels of nutrients and metals dissolved in the water column and adsorbed by suspended particulate matter [12].

The classical methodology reported in the literature for assessing urban trace metal emission rates is based on measurements at the inlet and outlet of wastewater treatment plants [6,26,36,52–55]. Local and regional variations are well known, even for emissions that enter WWTP, where they are treated and subsequently reduced before being discharged to receiving waters. The above cited studies are based on the same reduction rates for all WWTP and could be improved. Commonly accepted values for urban TM emission rates are shown in Table 3.

Table 3. Cu and Zn urban emission rates (mg/PE/d).

Cu	Zn	Source
6.0	35.0	[6]
3.2	18.0	[53]
-	7.45	[52]
8.5	46.0	[55]
8.5	10.0	This study

Urban loads to French rivers have shown a regular decrease in TM releases since the 1960s [54], while the metal consumption by population, technologies, etc. showed an opposite trend. This was an indication of improved long-term environmental efficiency for metal emissions in France. The decrease in metal emissions depended on the activity sector (urban, industrial, etc.). In addition, depending on the manufactured products used in construction (urban structures buildings, roof runoff, etc.), TM releases could differ from

region to region [6,53]. The more recent and representative values have been implemented in MicMod. Zn emission rates have been decreasing steadily since 2007, which justifies the value used in this study.

3.1.2. Soil Leaching Functions

Cu and Zn soil loads were calibrated on the basis of TM concentration measurements in the upper parts of the rivers in the Mosel watershed, where urban and industrial discharges are very low [28,29]. This procedure allows the estimation of TM load concentrations associated with different types of soil (cultures, grassland, and forest). Due to calibration with environmental measurements, this method gives good results for estimating soil leaching functions (loads entering the river system from the soil watershed). TM loads (fluxes) were calculated by multiplying the soil leaching function (mg/m^3), the soil occupation (km^2), and the specific water discharge ($m^3/km^2/s$).

The concentrations of Cu and Zn in the Mosel tributaries were analysed. Two representative monitoring stations (located upstream on the catchment) not impacted by urban and industrial releases were selected: Autrive on the Moselotte River (46.4 km from the source) and Thiebaumenil on the Vezouze River (53 km from the source), both tributaries of the Mosel River. Calibration was carried out at these monitoring stations (by comparisons between simulated and measured concentrations). Once calibrated, the soil load functions were 1 mg/m^3 for dissolved Cu, 0.5 mg/m^3 for particulate Cu, 4 mg/m^3 for dissolved Zn, and 2.5 mg/m^3 for particulate Zn. These functions, characterising TM loads from soils, were added to the database (including urban, industrial, and wastewater treatment plants) in order to carry out simulations.

Annual evolutions of Cu concentrations at these two monitoring stations are illustrated in the Supplementary Materials Section (Figures S1 and S2).

The Cu and Zn concentrations in Mosel tributaries were below the Environmental Quality Standards (EQS) [56]. The annual average of dissolved concentrations in the Moselotte were 0.9 mg/m^3 and 3.9 mg/m^3 for Cu and Zn, respectively. On the Vezouze, the annual averages of dissolved concentrations were 1.0 mg/m^3 and 3.2 mg/m^3 for Cu and Zn, respectively. The EQS values for Cu and Zn [57,58] are 1.4 mg/m^3 and 7.8 mg/m^3.

Among the different pressures on the catchment, soil loads were more important during high flow. During low flow, they were of the same order as urban emissions for copper. The median Cu fluxes at the Mosel outlet were 3678 g/j from urban releases and 3631 g/j from soil leaching during the low flow period (June to September). However, the median Zn fluxes at the Mosel outlet were characterised by a 2-fold ratio between urban releases (6007 g/j) and soil leaching (12,683 g/j). The zinc soil load functions need further calibration, using more monitored data from main rivers and their tributaries.

3.1.3. Settling Velocities

For adsorptive trace metals [40,59], suspended sediments play a significant role in their fate. Therefore, bed sediments can be a major sink or a source of trace metals [34,60]. TM concentrations are particularly sensitive to parameters such as settling velocity, critical stress values on bed sediments (deposition or erosion), as well as metal partitioning coefficients [61–63].

Settling velocity values were proposed in [10], among other parameters impacting TM behaviour. A settling velocity of 0.0001 m/s was indicated in [34], which is appropriate for suspended silts (<30 µm) and clay (<2 µm). Measured settling velocities were comparted with different prediction formulae [64]. Table 4 shows settling velocity values by grain size class [10,34,61,64]. These values cover several orders of magnitude. Mean values were calibrated in the MicMod sub-model.

Table 4. Settling velocity (m/s) associated with SS grain size (µm).

Settling Velocity Range (m/s)	Diameter (µm)	Source
1.0×10^{-6}–1.0×10^{-3} 1.0×10^{-5}–1.0×10^{-3}	Very fine SS [1] Fine SS [2]	[10]
9.0×10^{-6}–2.0×10^{-3}	-	[61]
1.0×10^{-4}	Silt < 30 µm Clay < 2 µm	[34]
5.7×10^{-7} 5.6×10^{-5} 1.4×10^{-3}	1 µm 10 µm 50 µm	[64]
9.3×10^{-6} 1.2×10^{-5} 2.3×10^{-5}	Clay < 2 µm Fine silt < 16 µm Coarse silt < 64 µm	This study

Note(s): 1 SS that exhibits very low settling velocity either because of its size or density. 2 SS prone to sedimentation, entering the river during high flow conditions.

Using the values from Table 4, Figure 3 shows the simulated annual evolution of particulate Cu concentrations adsorbed by clay, fine silt, and coarse silt (the annual evolution of particulate Zn concentrations is shown in Supplementary Materials, Figure S3). Due to the preferential trace metal adsorption by clay, the clay settling flux had a strong influence on particulate TM concentrations (Figure 4). The clay settling flux (expressed in $g/m^2/d$) occurred when flow velocity was sufficiently low (Supplementary Materials, Figure S4); the critical flow velocity at which clay can settle is considered to be ≤ 0.15 m/s. Fine silt settling flux occurred when flow velocity was lower than 0.3 m/s. When flow velocities were in the range of 0.15 and 0.3 m/s, fine silt preferentially settled, with higher settling fluxes when velocities were close to 0.15 m/s. When flow velocities were lower than 0.15 m/s, the load of fine silt sediments from the watershed decreased due to a decrease in specific discharges. The fine silt concentration in the water column also decreased. Below the threshold of 0.15 m/s, clay settling occurred and increased with decreasing flow velocities.

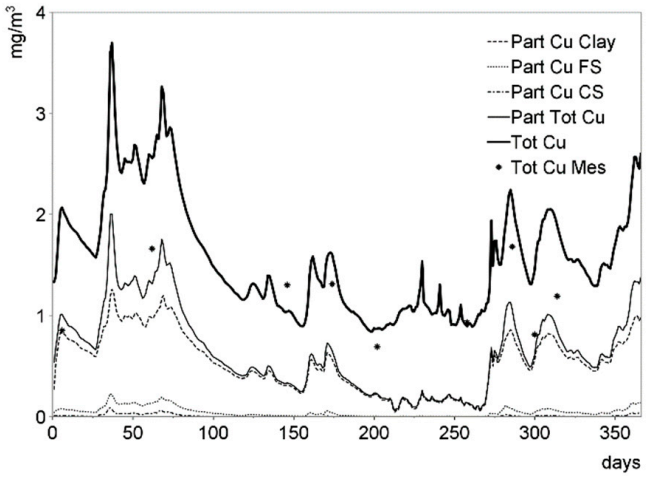

Figure 3. Time series of simulated particulate Cu concentrations adsorbed by clay (dashed curve), fine silt (dotted curve), and coarse silt (dotted-dashed curve); particulate Cu concentrations adsorbed by total SS (continued curve); total Cu concentrations (bold curve); and measured total Cu concentrations (dots) at Liverdun (193.5 km) on the Mosel River, year 2020.

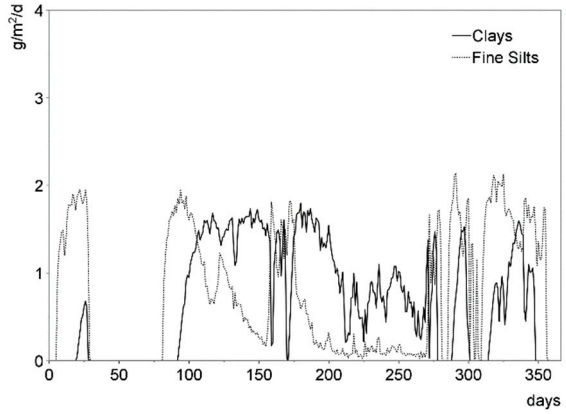

Figure 4. Time series of simulated settling fluxes ($g/m^2/d$) of clay (continued curve) and fine silt (dotted curve) at Liverdun (193.5 km) on the Mosel River, year 2020.

3.2. Characterisation of Trace Metal Dynamics with a Pressure–Impact Model

3.2.1. Assessment of Sediment Distribution by Class

The Meuse River was studied at the Eijsden monitoring station (617 km), located at the Belgo–Dutch border.

Suspended sediments and their associated grain sizes (clay, fine silt, coarse silt, and sand) can significantly influence the behaviour of trace metals in a river ecosystem. A prerequisite for simulating TM behaviour is an accurate representation of hydro-sedimentary processes. For each type of release (urban, industrial, and soil loads), the SS loads were distributed in each considered grain size class (clay, fine silt, etc.). The distribution between dissolved and particulate phases of TM was calculated according to SS concentrations and the Kd partitioning coefficient of each class, assuming fixed partitioning coefficients per class.

The SS concentrations simulated by the MicMod sub-model were compared to the observations at the Eijsden monitoring station. Time series comparisons of total SS concentrations and SS concentrations by class are presented for the year 2020 (Figure 5).

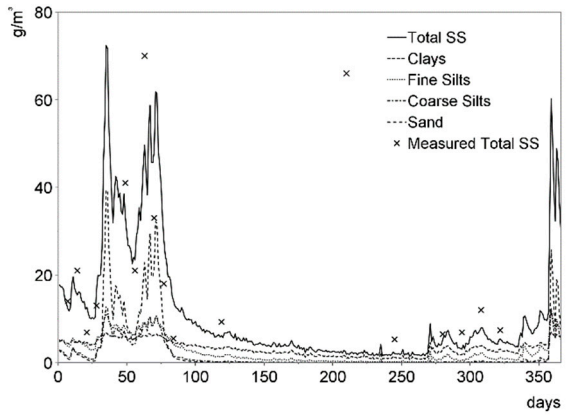

Figure 5. Time series of simulated total SS concentrations (g/m^3, continued curve); clay (dashed curve); fine silt (dotted curve); coarse silt (dotted-dashed curve); sand (small dashed curve); and measured total SS concentrations (crosses) in the water column at Eijsden (617 km) on the Meuse River (year 2020).

The simulated flow in the Meuse River at Eijsden (Supplementary Materials, Figure S5) provides the hydrological context. In the first approach, the simulated SS concentrations were well correlated with flow. The contribution of different particulate fractions was contrasted. The model showed that low flows were characterised by more clay relative to other sediment classes, while during high flows, the sand fraction increased. The sedimentation

period was identified during low flow conditions. Each class of sediment decreased, even the finest clay class when the flow velocity was sufficiently low ($\leq$0.15 m/s).

3.2.2. Trace Metal Contamination of the River Ecosystem (Sediment and Water Column)

Figure 6 shows the comparison between all simulated and measured Cu concentrations at the Eijsden monitoring station (on the Meuse River, during the year 2020). It indicates that the simulated total Cu concentrations during high flow (black dots) are almost constant (around 2 mg/m^3), while the measurements show variations between 1 and 5 mg/m^3. A similar effect, although less pronounced, is observed for Zn (Figure 7), where simulated values are above 7 mg/m^3, with most values around 10 mg/m^3, while measured values fluctuate between 4 and 20 mg/m^3. Considering low flow periods (coloured dots, Figure 6), the scatter plot was quite well aligned on the 1:1 line. Some discrepancies between simulated and observed Cu concentrations remained during high flow periods, where simulated concentrations were globally underestimated. The underestimation of Cu concentrations during high flow periods could be caused by an underestimation of particulate matter from soils by leaching. An increase in river discharges induced an increase in the coarse sediment fraction (>63 µm) in the river relative to the fine particle fractions (<63 µm) [65]. As the fine particle fraction carries TM, we focus on the low-flow conditions in this study. This is less obvious for Zn (Figure 7).

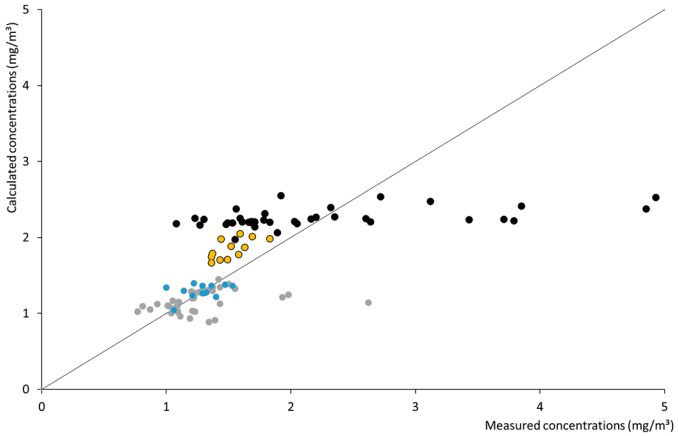

Figure 6. Comparison between all simulated and measured total and dissolved Cu concentrations (black and grey dots, respectively), and total and dissolved Cu concentrations during low flow conditions (yellow dots and blue dots, respectively), at the Eijsden monitoring station (617 km), year 2020.

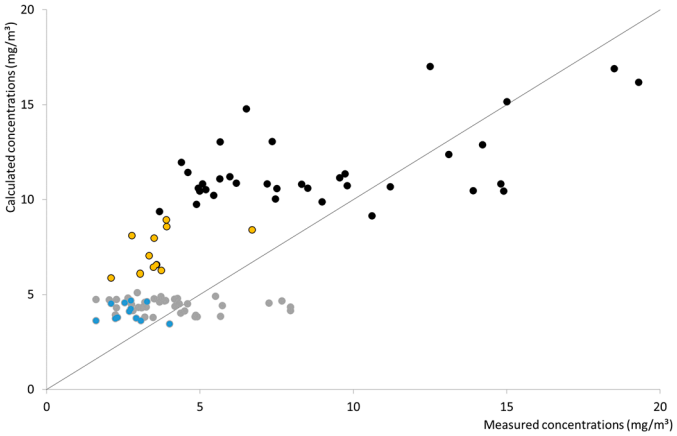

Figure 7. Comparison between all simulated and measured total and dissolved Zn concentrations (black and grey dots, respectively), and total and dissolved Zn concentrations during low flow conditions (yellow dots and blue dots, respectively), at the Eijsden monitoring station (617 km), year 2020.

The validation phase consisted of comparisons between the dissolved and total TM concentrations simulated by MicMod and the observations at the Eijsden monitoring station on the Meuse River. Time series comparisons of dissolved and total Cu concentrations are presented for the year 2020 (Figures 8 and 9; dissolved and total Zn concentrations are shown in the Supplementary Materials, Figures S6 and S7). The dissolved Cu concentrations were not influenced by the flow variations and were constant throughout the year. The simulation predicted an influence of hydrology, and consequently of SS concentrations, on total Cu and Zn concentrations. During January, February, and the end of the year, total Cu and Zn concentrations were variable. This was reflected in particulate Cu and Zn concentrations (Supplementary Material, Figures S8 and S9). The model expected that particulate Cu and Zn concentrations entering the river system would be lost by sedimentation during the low flow period (Supplementary Materials, Figure S10). Overall, simulated concentrations (SS and TM) during this period are within the range of observed values. Indeed, high flow was not well represented, probably due to the input of coarser particulate matter from soils. Total Zn concentrations showed a slight discrepancy between simulated and observed values (Supplementary Materials, Figure S7), probably due to a specific load dynamic during 2020 (from urban or soil emission rates). Nevertheless, they remained within the same order of magnitude as the observations. Since TM is mainly adsorbed by fine particles, this work focused on that fine grain size class.

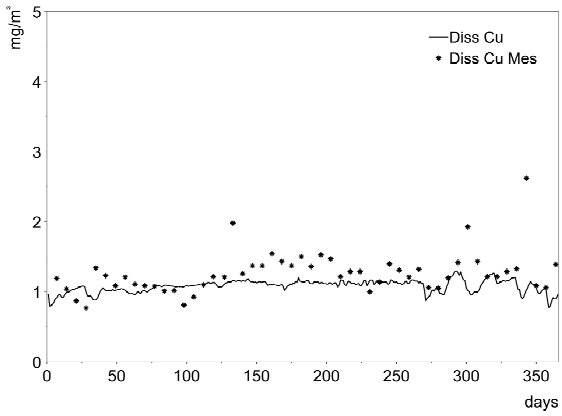

Figure 8. Time series of simulated dissolved Cu concentrations (mg/m^3, curve) and measured dissolved Cu concentrations (dots) at Eijsden (617 km) on the Meuse River, year 2020.

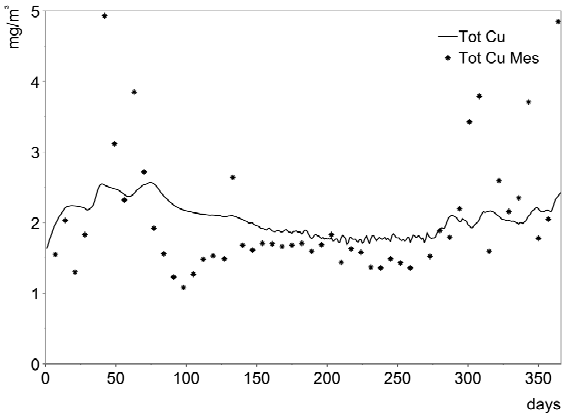

Figure 9. Time series of simulated total Cu concentrations (mg/m^3, curve) and measured total Cu concentrations (dots) at Eijsden (617 km) on the Meuse River, year 2020.

Some modelling studies have simulated TM transport for specific hydrological events over a few days [66] and under contrasting hydrology [10]. The simulations achieved in this paper are relevant for representing the annual period, with a focus on low flow

conditions, in order to validate the processes describing TM and SS behaviour in a large river system. The multi-class system description was analysed in terms of class distribution and associated grain size (cf. Section 3.4). The influence of Kd on the multi-class sediment system was also assessed (cf. Section 3.5).

3.3. Distribution by Class of Particulate Trace Metal

In the Meuse watershed, the distribution of particulate Cu on SS by class is shown in Figure 10 (Supplementary Materials, Figure S11: particulate Zn concentrations adsorbed by total SS, clay, fine silt, and coarse silt). Particulate TM were mainly adsorbed by clay. From June to September, all particulate TM were adsorbed by clay, as coarser sediments settled during the low flow period. This situation lasted during October and November. It was only from January to April and in December, during the high flow period, that other sediment fractions such as fine silt, supplied by drainage from the catchment, were available in the water column to adsorb particulate TM.

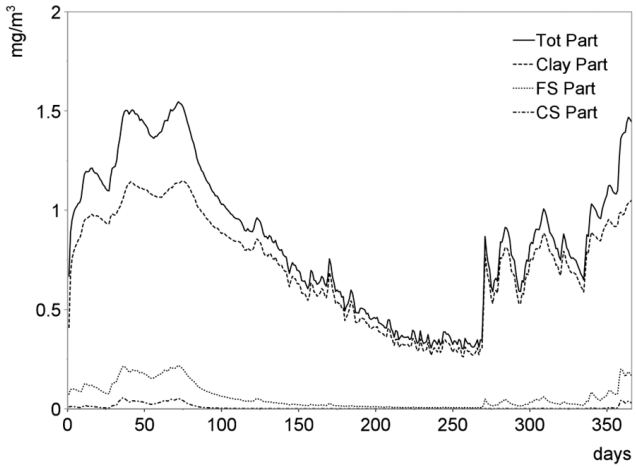

Figure 10. Time series of simulated particulate Cu concentrations adsorbed by total SS (mg/m^3, curve), clay (dashed curve), fine silt (dotted curve), and coarse silt (dotted-dashed curve) at Eijsden (617 km) on the Meuse River, year 2020.

3.4. Optimisation of the Suspended Sediments Modelling

The MicMod sub-model is composed of four classes of mineral suspended sediments: clay < 2 µm, 2 < fine silt < 16 µm, 16 < coarse silt < 64 µm, and 64 < sand < 250 µm. Fine SS classes control TM behaviour through adsorption and desorption processes, sedimentation on the riverbed, and resuspension in the water column. According to the flow, variable fractions of fine to coarse particles are implied in river dynamics, and TM fluxes are moved downstream by transport and vertically in the water column (to or from the bed layer).

The number of particle classes used to simulate SS heterogeneity, along with the associated class-specific parameters, have an impact on simulated dissolved and particulate TM concentrations. To evaluate this effect, comparisons were achieved between a one-class (1-class) and a four-classes (4-classes) SS model. The characterisation of the 1-class model is based on a "mean" particle, with a size of 63 µm, a settling velocity of 1.2×10^{-5} m/s, a Cu partitioning coefficient of 0.120 m^3/g, and a Zn partitioning coefficient of 0.175 m^3/g.

An additional simulation was conducted using a 1-class model with clay particles as the only SS, with a size equal to 1 µm, a settling velocity of 9.3×10^{-6} m/s, a Cu partitioning coefficient of 0.218 m^3/g, and a Zn partitioning coefficient of 0.391 m^3/g.

Figures 11 and 12 show that simulated dissolved Cu and Zn concentrations were higher with the 1-class mean particle model than with the 4-classes model. Simulated total Cu and Zn concentrations were higher with the 1-class mean particle model than with the 4-

classes model during the low flow period (Supplementary Materials, Figures S12 and S13). The 1-class model with clay particles shows Cu and Zn concentrations similar to those simulated by the 4-classes model, except for slight discrepancies during an intermediate period between April and July. The sedimentation process was well represented during low flow in the 1-class model with clay particles.

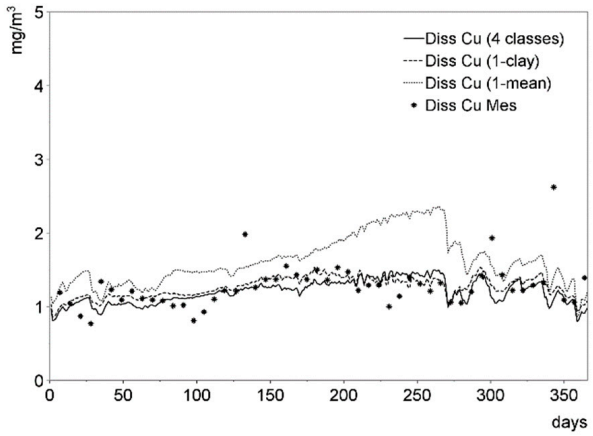

Figure 11. Time series of simulated dissolved Cu concentrations by the four-classes model (mg/m^3, continued curve), the one-class model with clay particles (dashed curve), the one-class model with mean particles (dotted curve), and measured dissolved Cu concentrations (dots) at Eijsden (617 km) on the Meuse River (year 2020).

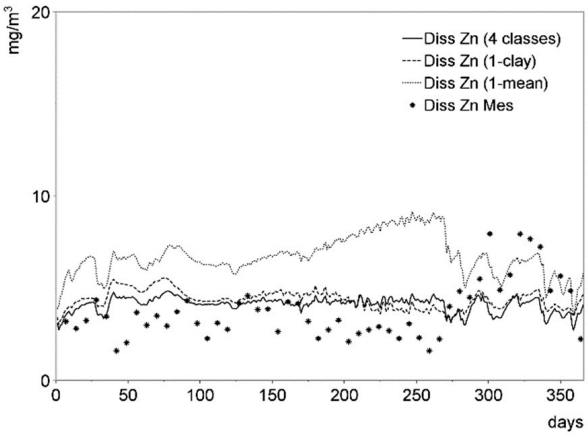

Figure 12. Time series of simulated dissolved Zn concentrations by the four-classes model (mg/m^3, continued curve), the one-class model with clay particles (dashed curve), the one-class model with mean particles (dotted curve), and measured dissolved Zn concentrations (dots) at Eijsden (617 km) on the Meuse River, year 2020.

Figure 13 shows the total SS concentrations simulated by the 4-classes model, the 1-class mean particle model, and the 1-class model with clay particles. It shows that the concentrations of mean particles and clay particles were comparable in terms of total SS concentrations. It also shows that coarser particles than clay must be taken into account during high flow conditions to accurately simulate SS concentrations.

Table 5 shows that the statistics (10th percentile, 50th percentile, and 90th percentile) of simulated TM concentrations are systematically overestimated with the 1-class mean particle model (compared to the results with the 4-classes system model). This demonstrates that TM concentrations were better characterised by the 4-classes system model.

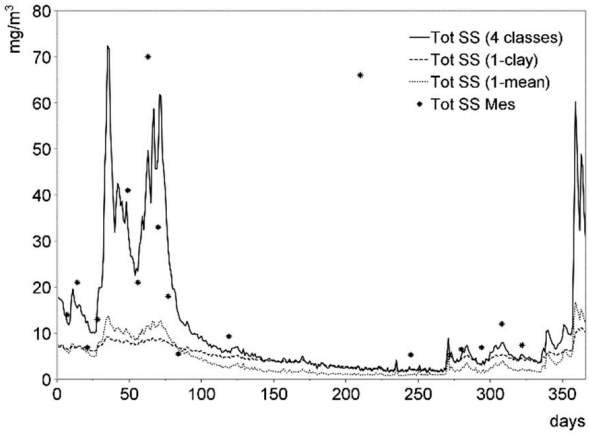

Figure 13. Time series of total SS concentrations simulated by the four-classes model (mg/m^3, continued curve), the one-class model with clay particles (dashed curve), the one-class model with mean particles (dotted curve), and measured total SS concentrations (dots) at Eijsden (617 km) on the Meuse River, year 2020.

Table 5. Statistics on simulated Cu and Zn concentrations with the 1-class mean particle model and the 4-classes system model.

	1-Class Model (Mean Particle)				4-Classes Model			
	Cu-d	**Cu-t**	**Zn-d**	**Zn-t**	**Cu-d**	**Cu-t**	**Zn-d**	**Zn-t**
P10	1.23	1.82	5.39	7.87	0.99	1.77	3.50	6.23
P50	1.55	2.02	6.62	8.78	1.21	2.04	4.21	8.90
P90	2.21	2.46	8.50	14.71	1.42	2.43	4.53	14.55

The modelling of particulate TM transport and sedimentation–erosion processes was better characterised using a grain size SS description with more than a single class. Using two classes is common [10,67] and provides acceptable results. The multi-class SS system with four size classes, developed in this work, showed good results for modelling particulate TM transport and erosion–sedimentation processes. More than the number of classes, the grain size and the associated parameters (partitioning coefficient, settling velocity, critical velocity from which particles can settle, etc.) characterising each grain size class were the most important prerequisites to ensure the best representation of the TM cycle in the river system.

3.5. Validation of SS and TM Modelling on Other Datasets

The copper and zinc partitioning coefficients were calibrated according to grain size (clay, fine silt, and coarse silt) in the Meuse River at the Eijsden monitoring station [16]. These Kd values have been used in environmental modelling dedicated to water quality assessment and have contributed to an explicit description of TM behaviour in the Meuse. The adsorption modelling hypothesis and associated Kd values were applied to another river basin (Mosel) with the same characteristics as the Meuse in terms of discharges, hydromorphology (canalised rivers), etc. Suspended sediments and trace metals concentrations were studied in the Mosel watershed at the Liverdun monitoring station (193.5 km on the Mosel River).

Within this new application, time series comparisons of dissolved and total Cu concentrations at the monitoring station are presented for the year 2020 (Figures 14 and 15). Dissolved and total Zn are shown in the Supplementary Materials Section (Figures S14 and S15). The simulated flow of the Mosel River at Liverdun (Supplementary Materials, Figure S16) provides the hydrological context. The simulated SS concentrations (Supplementary Materials,

Figure S17) were well correlated with the flow. The simulation predicted a slight influence of hydrology on total Cu and Zn concentrations. Dissolved Cu and Zn concentrations were not influenced by flow variations and were relatively constant throughout the year. High variability in flow conditions was observed from January to May and from November to December. This is reflected in the particulate Cu and Zn concentrations (Supplementary Materials, Figures S18 and S19). The model expected that the particulate Cu and Zn concentrations entering the river system were lost by sedimentation (Supplementary Materials, Figure S20). Overall, simulated concentrations were in the range of observed values during low flow conditions. The multi-class SS system (four size classes) produced good results for modelling particulate TM transport and erosion–sedimentation processes on the Mosel River.

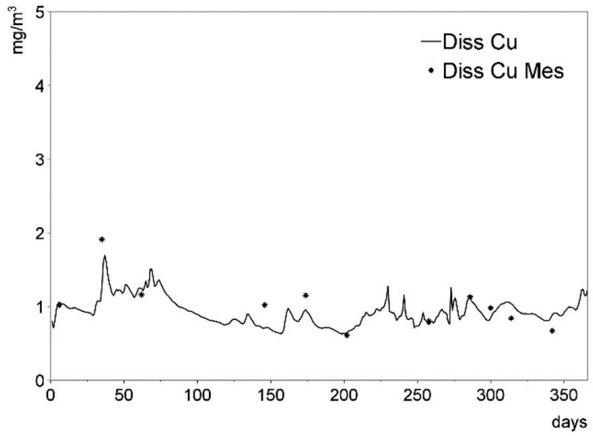

Figure 14. Time series of simulated dissolved Cu concentrations (mg/m^3, curve) and measured dissolved Cu concentrations (dots) at Liverdun on the Mosel River (193.5 km), year 2020.

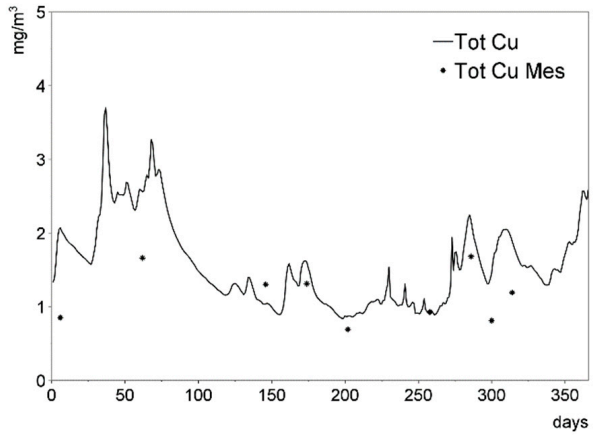

Figure 15. Time series of simulated total Cu concentrations (mg/m^3, curve) and measured total Cu concentrations (dots) at Liverdun on the Mosel River (193.5 km), year 2020.

This confirms the conclusion of [16] that Kd calibration is mainly influenced by hydro-sedimentary dynamics and grain size characterisation: a detailed description of grain size distribution allows better characterisation of particulate TM partitioning on SS and more accurate calibration of partitioning coefficients.

4. Conclusions

An assessment was performed on the interactions between trace metals and mineral suspended sediments using a deterministic description of hydro-sedimentary processes, including a multi-class sediment system. The MicMod sub-model simulated the behaviour of SS and TM, involving their transport and fate in the river ecosystem. The French part of the Mosel River and the Belgian part of the Meuse River were the first to be studied.

Dissolved and particulate copper and zinc concentrations were calculated in different configurations of SS classes along these two river stretches.

Previous calibrations of TM partitioning coefficients were used and enhanced, particularly for the Mosel watershed. The point and diffuse emissions were found to be significantly different at local and regional levels. Diffuse loads were associated with rainy periods and high flow conditions. The investigation focused on Cu and Zn loads from soil leaching. Dissolved and particulate TM concentrations were characterised using measurements in the upper parts of the Mosel watershed. We focused on low flow periods, which are more suitable for the transport of fine particle fractions. Other sources of TM were considered and calibrated: (i) urban emission rates from anthropogenic activities in the Meuse watershed and (ii) settling velocities described by grain size classes. A compilation of the literature was presented to establish a review of settling velocity values according to grain size class.

Suspended sediment, Cu, and Zn modelling were studied and characterised for the Meuse and Mosel basins, with the aim of providing a good description of pressure–impact relationships. This strengthens the capacity of the model to support water quality management in accordance with the European WFD.

The coupled modelling of SS and TM was intrinsically associated with a better representation of TM behaviour in river ecosystems. It was demonstrated that a description of at least one class of fine particles is necessary to adequately represent TM concentrations. A description of four classes (with one fine particle class < 2 μm and one coarse class > 150 μm) provided more suitable results. It is evident that these considerations contribute to enhancing the compliance of MicMod with WFD applications.

It was necessary to improve the knowledge of SS transport mechanisms in the context of a physico-chemical water quality survey at the holistic watershed scale, in order to describe TM transport. This has consequently led to a better understanding and modelling of aquatic ecosystems. The issue of partitioning coefficients and their role in the modelling approach has been thoroughly addressed. It has enabled the extension of water quality assessment from monitoring stations (measured data) to a spatially and temporally distributed diagnosis (with calculated concentrations available anywhere and at any time within the modelled river network).

It could be interesting to evaluate (i) the MicMod sub-model and its associated methodology at other monitoring stations, and (ii) the input of TM and SS from the tributaries of the Meuse River (i.e., the Geul River), in order to refine calibration under various conditions (hydromorphology, hydrology, and pressures), while also considering local specificities.

Supplementary Materials: The following supporting information can be downloaded at: https://www.mdpi.com/article/10.3390/w17131876/s1, Figure S1: Time series of simulated dissolved Cu concentrations (mg/m^3, curve) and measured dissolved Cu concentrations (dots) at Autrive (46.4 km) on the Moselotte River (year 2020). Figure S2: Time series of simulated dissolved Cu concentrations (mg/m^3, curve) and measured dissolved Cu concentrations (dots) at Thiebaumesnil (53 km) on the Vezouze River (year 2020). Figure S3: Time series of simulated particulate Zn concentrations adsorbed by clay (dashed curve), fine silt (dotted curve), and coarse silt (dotted-dashed curve); particulate Zn concentrations adsorbed by total SS (continued curve), total Zn concentrations (bold curve); and measured total Zn concentrations (dots) at Liverdun (193.5 km) on the Mosel River, year 2020. Figure S4: Time series of flow velocity (m/s) at Liverdun (193.5 km) on the Mosel River, year 2020. Figure S5: Time series of simulated flows (m^3/s) at Eijsden (617 km) on the Meuse River, year 2020. Figure S6: Time series of simulated dissolved Zn concentrations (mg/m^3, curve) and measured dissolved Zn concentrations (dots) at Eijsden (617 km) on the Meuse River, year 2020. Figure S7: Time series of simulated total Zn concentrations (mg/m^3, curve) and measured total Zn concentrations (dots) at Eijsden (617 km) on the Meuse River, year 2020. Figure S8: Time series of simulated total

Cu concentrations (mg/m^3, continued curve) and simulated particulate Cu concentrations (dashed curve) at Eijsden (617 km) on the Meuse River, year 2020. Figure S9: Time series of simulated total Zn concentrations (mg/m^3, continued curve) and simulated particulate Zn concentrations (dashed curve) at Eijsden (617 km) on the Meuse River, year 2020. Figure S10: Time series of simulated settling fluxes (g/m^2/d) of clay (continued curve) and fine silt (dotted curve) at Eijsden (617 km) on the Meuse River (year 2020). Figure S11: Time series of simulated particulate Zn concentrations adsorbed by total SS (mg/m^3, curve), clay (dashed curve), fine silt (dotted curve), and coarse silt (dotted-dashed curve) at Eijsden (617 km) on the Meuse River, year 2020. Figure S12: Time series of simulated total Cu concentrations by the four-classes model (mg/m^3, continued curve), one-class model with clay particles (dashed curve), one-class model with mean particles (dotted curve), and measured total Cu concentrations (dots) at Eijsden (617 km) on the Meuse River (year 2020). Figure S13: Time series of simulated total Zn concentrations by the four-classes model (mg/m^3, continued curve), one-class model with clay particles (dashed curve), one-class model with mean particles (dotted curve), and measured total Zn concentrations (dots) at Eijsden (617 km) on the Meuse River (year 2020). Figure S14: Time series of simulated dissolved Zn concentrations (mg/m^3, curve) and measured dissolved Zn concentrations (dots) at Liverdun on the Mosel River (193.5 km), year 2020. Figure S15: Time series of simulated total Zn concentrations (mg/m^3, curve) and measured total Zn concentrations (dots) at Liverdun on the Mosel River (193.5 km), year 2020. Figure S16: Time series of simulated flows (m^3/s) at Liverdun (193.5 km) on the Mosel River, year 2020. Figure S17: Time series of simulated total SS concentrations (g/m^3, continued curve), clay (dashed curve), fine silt (small dashed curve), coarse silt (dotted-dashed curve), sand (dotted curve), and measured total SS concentrations (g/m^3, black crosses) in the water column at Liverdun (193.5 km) on the Mosel River (year 2020). Figure S18: Time series of simulated total Cu concentrations (mg/m^3, dashed curve), simulated particulate Cu concentrations (continued curve), and total measured Cu concentrations (dots) at Liverdun (193.5 km) on the Mosel River, year 2020. Figure S19: Time series of simulated total Zn concentrations (mg/m^3, dashed curve), simulated particulate Zn concentrations (continued curve), and total measured Zn concentrations (dots) at Liverdun (193.5 km) on the Mosel River, year 2020. Figure S20: Time series of simulated settling fluxes (g/m^2/d) of clay (continued curve) and fine silt (dotted curve) at Liverdun (193.5 km) on the Mosel River (year 2020). Equations S1: First-order processes such as adsorption, desorption, sedimentation, resuspension, and discharges from the watershed described in the water column and suspended sediments.

Author Contributions: Investigation, A.G.; validation, A.G.; writing—original draft: A.G.; project administration, J.-F.D.; supervision, J.-F.D.; conceptualization, J.-F.D. and A.G.; methodology, J.-F.D. and A.G.; writing—review and editing, J.-F.D. and A.G. All authors have read and agreed to the published version of the manuscript.

Funding: This research received external funding (aid agreement for cooperation in scientific research, Pegase Opera) from French Water Agencies and self-funding.

Institutional Review Board Statement: Not applicable.

Informed Consent Statement: Not applicable.

Data Availability Statement: The Rhine–Meuse Water Agency, France (https://www.eau-rhin-meuse.fr/, accessed on 13 March 2023); the Rijkswaterstaat, The Netherlands (https://www.rijkswaterstaat.nl/, accessed on 9 May 2023).

Acknowledgments: The authors wish to express their thanks to the administration that made this study possible: the Rhine–Meuse Water Agency, France.

Conflicts of Interest: The authors declare no conflicts of interest.

Abbreviations

AERM	Agence de l'Eau Rhin-Meuse
BS	Bed sediment
C	Clay
CS	Coarse silt
FS	Fine silt
Kd	Partitioning coefficient
MicMod	Micropollutant modelling
POMD	Processes of organic matter degradation
RWS	Rijkswaterstaat
SPW	Service public wallon
SS	Suspended sediment
TM	Trace metal
WFD	Water Framework Directive 2000/60/EC
WWTP	Waste water treatment plant

References

1. Meybeck, M.; Lestel, L.; Bonté, P.; Moilleron, R. Historical Perspective of Heavy Metals Contamination (Cd, Cr, Cu, Hg, Pb, Zn) in the Seine River Basin (France) Following a DPSIR Approach (1950–2005). *Sci. Total Environ.* **2007**, *375*, 204–231. [CrossRef]
2. Gaillardet, J.; Viers, J.; Dupré, B. Trace Elements in River Waters. In *Treatise on Geochemistry*; Drever, J.I., Ed.; Surface and Ground Water, Weathering, Erosion and Soils; Elsevier: Amsterdam, The Netherlands, 2004; Volume 5, pp. 225–272. ISBN 978-0-08-098300-4.
3. Yang, Z.; Wang, Y.; Shen, Z.; Niu, J.; Tang, Z. Distribution and Speciation of Heavy Metals in Sediments from the Mainstream, Tributaries, and Lakes of the Yangtze River Catchment of Wuhan, China. *J. Hazard. Mater.* **2008**, *166*, 1186–1194. [CrossRef] [PubMed]
4. Meybeck, M. Man and River Interface: Multiple Impacts on Water and Particulates Chemistry Illustrated in the Seine River Basin. *Hydrobiologia* **1998**, *373*, 1–20. [CrossRef]
5. Ollivier, P.; Hamelin, B.; Radakovitch, O. Seasonal Variations of Physical and Chemical Erosion: A Three-Year Survey of the Rhone River (France). *Geochim. Cosmochim. Acta* **2010**, *74*, 907–927. [CrossRef]
6. Thévenot, D.; Moilleron, R.; Lestel, L.; Gromaire, M.-C.; Rocher, V.; Cambier, P.; Bonté, P.; Colin, J.-L.; Pontevès, C.; Meybeck, M. Critical Budget of Metal Sources and Pathways in the Seine River Basin (1994–2003) for Cd, Cr, Cu, Hg, Ni, Pb and Zn. *Sci. Total Environ.* **2007**, *375*, 180–203. [CrossRef] [PubMed]
7. Carone, M.T.; Simoniello, T.; Manfreda, S.; Caricato, G. Watershed Influence on Fluvial Ecosystems: An Integrated Methodology for River Water Quality Management. *Environ. Monit. Assess.* **2009**, *152*, 327–342. [CrossRef]
8. Dou, M.; Li, G.; Li, C. Quantitative Relations between Chemical Oxygen Demand Concentration and Its Influence Factors in the Sluice-Controlled River Reaches of Shaying River, China. *Environ. Monit. Assess.* **2014**, *187*, 4139. [CrossRef] [PubMed]
9. Zhang, Q.; Li, Z.; Zeng, G.; Li, J.; Fang, Y.; Yuan, Q.; Wang, Y.; Ye, F. Assessment of Surface Water Quality Using Multivariate Statistical Techniques in Red Soil Hilly Region: A Case Study of Xiangjiang Watershed, China. *Environ. Monit. Assess.* **2009**, *152*, 123–131. [CrossRef]
10. Garneau, C.; Sauvage, S.; Sánchez-Pérez, J.-M.; Lofts, S.; Brito, D.; Neves, R.; Probst, A. Modelling Trace Metal Transfer in Large Rivers under Dynamic Hydrology: A Coupled Hydrodynamic and Chemical Equilibrium Model. *Environ. Model. Softw.* **2017**, *89*, 77–96. [CrossRef]
11. Guéguen, C.; Dominik, J. Partitioning of Trace Metals between Particulate, Colloidal and Truly Dissolved Fractions in a Polluted River: The Upper Vistula River (Poland). *Appl. Geochem.* **2003**, *18*, 457–470. [CrossRef]
12. Dendievel, A.-M.; Grosbois, C.; Ayrault, S.; Evrard, O.; Coynel, A.; Debret, M.; Gardes, T.; Euzen, C.; Schmitt, L.; Chabaux, F.; et al. Key Factors Influencing Metal Concentrations in Sediments along Western European Rivers: A Long-Term Monitoring Study (1945–2020). *Sci. Total Environ.* **2022**, *805*, 149778. [CrossRef] [PubMed]
13. Directive 2000/60/EC of the European Parliament and of the Council of 23 October 2000 Establishing a Framework for Community Action in the Field of Water Policy. *Off. J. Eur. Communities* **2000**, *327*, 72. Available online: https://eur-lex.europa.eu/legal-content/EN/TXT/PDF/?uri=OJ:L:2000:327:FULL&from=EN (accessed on 20 June 2025).
14. Viers, J.; Dupré, B.; Gaillardet, J. Chemical Composition of Suspended Sediments in World Rivers: New Insights from a New Database. *Sci. Total Environ.* **2008**, *407*, 853–868. [CrossRef]
15. Meybeck, M. Heavy Metal Contamination in Rivers across the Globe: An Indicator of Complex Interactions between Societies and Catchments. *IAHS-AISH Proc. Rep.* **2013**, *361*, 3–16.

16. Grard, A.; Deliège, J.-F. Characterizing Trace Metal Contamination and Partitioning in the Rivers and Sediments of Western Europe Watersheds. *Hydrology* **2023**, *10*, 51. [CrossRef]
17. Deliège, J.-F.; Everbecq, E.; Magermans, P.; Grard, A.; Bourouag, T.; Blockx, C. Pegase, A Software Dedicated to Surface Water Quality Assessment and to European Database Reporting. In Proceedings of the European conference of the Czech Presidency of the Council of the EU Towards Environment, Opportunities of SEIS and SIZE: Integrating Environmental Knowledge in Europe, Brno, Czech Republic, 1 January 2009; pp. 24–32.
18. Commission Internationale de La Meuse (CIM). *District Hydrographique International de La Meuse-Analyse, Rapport Faîtier*; Commission Internationale de La Meuse: Liège, Belgium, 2005; Available online: http://www.meuse-maas.be (accessed on 20 June 2025).
19. Etat de l'Environnement Wallon. Direction de l'Etat Environnemental. SPW. 2021. Available online: http://etat.environnement.wallonie.be/contents/indicatorsheets/EAU%202.html (accessed on 12 October 2022).
20. Agence de l'Eau Rhin-Meuse. Caractéristiques et Priorités Dans La Territoire D'Interventions Moselle Amont. 2003. Available online: https://www.documentation.eauetbiodiversite.fr/ (accessed on 20 June 2025).
21. Waterinfo, Rijkswaterstaat, Ministerie van Infrastructuur En Waterstaat. Available online: https://waterinfo.rws.nl (accessed on 7 July 2021).
22. INRAE (Institut National de Recherche Pour l'Agriculture, l'Alimentation et l'Environnement, Antony, France): The Sunshine Web Apps. Available online: https://sunshine.inrae.fr/app/profilsHydro (accessed on 12 October 2022).
23. HydroPortail-Eaufrance. Available online: https://www.hydro.eaufrance.fr/ (accessed on 20 June 2025).
24. Syndicat Mixte Moselle Aval. Dossier de Candidature à la Labellisation «Programme d'Actions de Prévention des Inondations (PAPI)». 2019. Available online: https://www.moselleaval.fr/fr/accueil.html (accessed on 15 October 2022).
25. Knöchel, A. Book Review: Cation Binding by Humic Substances By Edward Tipping. *Angew. Chem. Int. Ed.* **2003**, *42*, 2817. [CrossRef]
26. Etat Des Lieux. Éléments de Diagnostic de La Partie Française Du District Du Rhin et Du District de La Meuse. Adopté Au Comité de Bassin de l'Agence de l'Eau Rhin-Meuse. 2019. Available online: https://www.eau-rhin-meuse.fr/etat-des-lieux-des-districts-du-rhin-et-de-la-meuse (accessed on 20 June 2025).
27. Naïades-Données Sur La Qualité Des Eaux de Surface. Available online: https://naiades.eaufrance.fr/ (accessed on 10 June 2023).
28. Deliège, J.-F. Méthode d'Intégration de Modèles Adaptée Aux Systèmes Hydrologiques Multicompartimentés. Ph.D. Thesis, Université de Liège, Liège, Belgium, 2013.
29. Everbecq, E.; Grard, A.; Magermans, P.; Deliège, J.-F. Water Framework Directive and Modelling Using PEGOPERA Simulation Software. *J. Model. Optim.* **2019**, *11*, 36–50. [CrossRef]
30. Pelletier, G.J.; Chapra, S.C.; Tao, H. QUAL2Kw—A Framework for Modeling Water Quality in Streams and Rivers Using a Genetic Algorithm for Calibration. *Environ. Model. Softw.* **2006**, *21*, 419–425. [CrossRef]
31. Wool, T.; Ambrose, R.B.; Martin, J.L.; Comer, A. WASP 8: The Next Generation in the 50-Year Evolution of USEPA's Water Quality Model. *Water* **2020**, *12*, 1398. [CrossRef]
32. Park, R.A.; Clough, J.S.; Wellman, M.C. AQUATOX: Modeling Environmental Fate and Ecological Effects in Aquatic Ecosystems. *Ecol. Model.* **2008**, *213*, 1–15. [CrossRef]
33. Owens, P.N.; Petticrew, E.L. Bernd Westrich, Ulrich Förstner (Eds.): Sediment Dynamics and Pollutant Mobility in Rivers—An Interdisciplinary Approach. *J. Soils Sediments* **2008**, *8*, 151–153. [CrossRef]
34. Trento, A.; Álvarez, A. A Numerical Model for the Transport of Chromium and Fine Sediments. *Environ. Model. Assess.* **2011**, *16*, 551–564. [CrossRef]
35. Tercier-Waeber, M.-L.; Stoll, S.; Slaveykova, V.I. Trace Metal Behavior in Surface Waters: Emphasis on Dynamic Speciation, Sorption, Processes and Bioavailability. *Arch. Sci. Ed. Société Phys. D'histoire Nat. Genève* **2012**, *65*, 119–142.
36. Coquery, M.; Miege, C.; Choubert, J.M.; Ruel, S.M.; Gabet, V.; Lardy, S.; Esperanza, M.; Budzinski, H. Projet AMPERES: Analyse de micropolluants prioritaires et émergents dans les rejets et les eaux superficielles. In Proceedings of the 5èmes Journées Techniques Eaux et Déchets, Toulouse, France, 11 June 2008; p. 19.
37. Chang, C.-L.; Yu, Z.-E. Application of Water Quality Model to Analyze Pollution Hotspots and the Impact on Reservoir Eutrophication. *Environ. Monit. Assess.* **2020**, *192*, 495. [CrossRef]
38. Wan, L.; Wang, H. Control of Urban River Water Pollution Is Studied Based on SMS. *Environ. Technol. Innov.* **2021**, *22*, 101468. [CrossRef]
39. Hatten, J.; Goni, M.; Wheatcroft, R. Chemical Characteristics of Particulate Organic Matter from a Small, Mountainous River System in the Oregon Coast Range, USA. *Biogeochemistry* **2012**, *107*, 43–66. [CrossRef]
40. Li, R.; Tang, C.; Cao, Y.; Jiang, T.; Chen, J. The Distribution and Partitioning of Trace Metals (Pb, Cd, Cu, and Zn) and Metalloid (As) in the Beijiang River. *Environ. Monit Assess* **2018**, *190*, 399. [CrossRef]

41. Grard, A.; Everbecq, E.; Magermans, P.; Deliège, J.-F. Modelling a Severe Transient Anoxia of Continental Freshwaters Due to a Scheldt Accidental Release (Sugar Industry). *Hydrology* **2021**, *8*, 175. [CrossRef]
42. Fournier, J.; Bonnot-Courtois, C.; Paris, R.; Vot, M. *Analyses Granulométriques. Principes et Méthodes*; CNRS: Dinard, France, 2012; p. 100.
43. Wentworth, C.K. A Scale of Grade and Class Terms for Clastic Sediments. *J. Geol.* **1922**, *30*, 377–392. [CrossRef]
44. Friedman, G.M.; Sanders, J.B. Principles of Sedimentology. *J. Sediment. Petrol.* **1979**, *49*, 679–680.
45. Blott, S.J.; Pye, K. GRADISTAT: A Grain Size Distribution and Statistics Package for the Analysis of Unconsolidated Sediments. *Earth Surf. Process. Landf.* **2001**, *26*, 1237–1248. [CrossRef]
46. Everbecq, E.; Grard, A.; Magermans, P.; Deliège, J.-F. Pegase: Description des Paramètres du Modèle Pegase. Rapport de Recherche Interne. 2022. Available online: https://orbi.uliege.be/handle/2268/198392 (accessed on 20 June 2025).
47. Tipping, E. Humic Ion-Binding Model VI: An Improved Description of the Interactions of Protons and Metal Ions with Humic Substances. *Aquat. Geochem.* **1998**, *4*, 3–47. [CrossRef]
48. Ollivier, P.; Radakovitch, O.; Hamelin, B. Major and Trace Element Partition and Fluxes in the Rhône River. *Chem. Geol.* **2011**, *285*, 15–31. [CrossRef]
49. Zhang, J.; Huang, W.W.; Wang, J.H. Trace-Metal Chemistry of the Huanghe (Yellow River), China—Examination of the Data from in Situ Measurements and Laboratory Approach. *Chem. Geol.* **1994**, *114*, 83–94. [CrossRef]
50. Ciffroy, P.; Durrieu, G.; Garnier, J.-M. Probabilistic Distribution Coefficients (Kds) in Freshwater for Radioisotopes of Ag, Am, Ba, Be, Ce, Co, Cs, I, Mn, Pu, Ra, Ru, Sb, Sr and Th—Implications for Uncertainty Analysis of Models Simulating the Transport of Radionuclides in Rivers. *J. Environ. Radioact.* **2009**, *100*, 785–794. [CrossRef]
51. Deliège, J.; Everbecq, E.; Magermans, P.; Grard, A.; Bourouag, T.; Blockx, C. Pegase, An Integrated River/Basin Model Dedicated to Surface Water Quality Assessment: Application to Cocaine Environmental and Industrial Toxicology. *Acta Clin. Belg.* **2010**, *65*, 42–48. [CrossRef]
52. RSDE—Campagnes. Analyses Des Résultats Sur Les Bassins Rhône-Méditerranée et Corse. Synthèse (Mars 2020). Agence de l'eau Rhône Méditerranée Corse. Available online: https://www.eaurmc.fr/jcms/pro_99324/fr/rsde-campagnes-2018-analyses-des-resultats-sur-les-bassins-rhone-mediterranee-et-corse (accessed on 20 June 2025).
53. Le, N.D. Relations Entre La Variabilité de La Pollution Urbaine et Le Contexte Socio-Culturel Du Bassin de Collecte. Ph.D. Thesis, Université de Lorraine, Lorraine, France, 2013.
54. Ayrault, S.; Meybeck, M.; Mouchel, J.-M.; Gaspéri, J.; Lestel, L.; Lorgeoux, C.; Boust, D. Sedimentary Archives Reveal the Concealed History of Micropollutant Contamination in the Seine River Basin. In *The Seine River Basin*; Flipo, N., Labadie, P., Lestel, L., Eds.; The Handbook of Environmental Chemistry; Springer International Publishing: Cham, Switzerland, 2021; pp. 269–300. ISBN 978-3-030-54260-3. [CrossRef]
55. Everbecq, E.; Bourouag, M.; Grard, A.; Deliège, J.-F.; Smitz, J. *Uitvoeren van een Studie voor de Risico-Analyse 2015 in Het Scheldestroomgebied met Behulp van het PEGASE-Model van het Scheldestroomgebied: Derde Technisch-Wetenschappelijk Rapport-Zware metalen en Zwevende Stoffen Modellering*; Vlaamse MilieuMaatschappij: Brussels, Belgium, 2008.
56. Bass, J.A.B.; Blust, R.; Clarke, R.T.; Corbin, T.A.; Davison, W.; de Schamphelaere, K.A.C.; Janssen, C.R.; Kalis, E.J.J.; Kelly, M.G.; Kneebone, N.T.; et al. Environmental Quality Standards for Trace Metals in the Aquatic Environment. *Environ. Agency* **2008**, *177*, SC030194.
57. Agence de l'Eau Seine-Normandie. *Guide Pratique Des Micropolluants Dans Les Eaux Du Bassin Seine-Normandie*; Agence de l'Eau Seine-Normandie: Courbevoie, France, 2018.
58. INERIS. Données Technico-Économiques Sur Les Substances Chimiques En France: Cuivre, Composés et Alliages. DRC-14-136881-02236A. 2014. Available online: https://substances.ineris.fr/sites/default/files/archives/7440-50-8%20--%20Cuivre%20--%20FTE.pdf (accessed on 20 June 2025).
59. Pertsemli, E.; Voutsa, D. Distribution of Heavy Metals in Lakes Doirani and Kerkini, Northern Greece. *J. Hazard. Mater.* **2007**, *148*, 529–537. [CrossRef]
60. Liu, W.-C.; Chen, W.-B.; Chang, Y.-P. Modeling the Transport and Distribution of Lead in Tidal Keelung River Estuary. *Environ. Earth Sci.-Environ. Earth Sci.* **2012**, *65*, 39–47. [CrossRef]
61. Cho, E.; Arhonditsis, G.B.; Khim, J.; Chung, S.; Heo, T.-Y. Modeling Metal-Sediment Interaction Processes: Parameter Sensitivity Assessment and Uncertainty Analysis. *Environ. Model. Softw.* **2016**, *80*, 159–174. [CrossRef]
62. Chalov, S.; Moreido, V.; Sharapova, E.; Efimova, L.; Efimov, V.; Lychagin, M.; Kasimov, N. Hydrodynamic Controls of Particulate Metals Partitioning Along the Lower Selenga River—Main Tributary of The Lake Baikal. *Water* **2020**, *12*, 1345. [CrossRef]
63. Dietrich, W.E. Settling Velocity of Natural Particles. *Water Resour. Res.* **1982**, *18*, 1615–1626. [CrossRef]
64. Cheng, N.-S. Simplified Settling Velocity Formula for Sediment Particle. *J. Hydraul. Eng.-ASCE* **1997**, *123*, 149–152. [CrossRef]
65. Vilmin, L.; Aissa-Grouz, N.; Garnier, J.; Billen, G.; Mouchel, J.-M.; Poulin, M.; Flipo, N. Impact of Hydro-Sedimentary Processes on the Dynamics of Soluble Reactive Phosphorus in the Seine River. *Biogeochemistry* **2015**, *122*, 229–251. [CrossRef]

66. Lindenschmidt, K.-E.; Wodrich, R.; Hesse, C. The Effects of Scaling and Model Complexity in Simulating the Transport of Inorganic Micropollutants in a Lowland River Reach. *Water Qual. Res. J. Can.* **2006**, *41*, 24–36. [CrossRef]
67. El Ganaoui Mourlan, O.; Schaaff, E.; Boyer, P.; Amielh, M.; Anselmet, F.; Grenz, C. The Deposition and Erosion of Cohesive Sediments Determined by a Multi-Class Model. *Estuar. Coast. Shelf Sci.* **2004**, *60*, 457–475. [CrossRef]